

Article

Variations in Glacier Runoff Contributed by the Increased Negative Mass Balance over the Last Forty Years in the Tien Shan Mountains

Hongyu Wang , Changchun Xu * , Gang Ying, Fang Liu  and Yunxia Long

Xinjiang Key Laboratory of Oasis Ecology, College of Geographical Science, Xinjiang University, Urumqi 830017, China; why96@stu.xju.edu.cn (H.W.); chinayg@xju.edu.cn (G.Y.); lf_1900666@stu.xju.edu.cn (F.L.); lyx818@stu.xju.edu.cn (Y.L.)

* Correspondence: xcc0110@163.com

Abstract: In the context of global warming, the melting of glaciers in the Tien Shan Mountains as the important “solid reservoir” in the arid area of Central Asia is accelerating in recent decades, leading to profound changes in regional water resources. Based on the simulated glaciological data from the Python Glacier Evolution Model (PyGEM) and the measured glaciological data from the World Glacier Monitoring Service (WGMS), this paper analyzed the applicability of simulated data, the changes in glacier mass balance, and the responses of the glacier to climate change and its impacts on glacier runoff in the Tien Shan Mountains. The results show that (1) the PyGEM simulation dataset is in good agreement with the measurements, which can effectively reproduce the change in the glacier mass balance in the Tien Shan Mountains glaciers and is suitable for studying the regional scale glacier change. (2) From 1980 to 2016, the decadal average mass balance change rate of glaciers in the Tien Shan Mountains was -0.012 m w.e. yr^{-1} . The regional mass balance showed an overall negative increasing trend (the area with increasingly negative accounted for 80.13% of the entire area), with a positive increase that only occurred in the West Tien Shan Mountains and western North Tien Shan Mountains (19.87%). (3) The correlation between the temperature and mass balance is much higher than that between the precipitation and mass balance. Temperature dominates the change and development of regional glaciers. The increase in negative glacier mass balance that was observed in the study area is mainly affected by the rising temperature, the decreasing solid precipitation in the accumulation period, and the rapid melting in the ablation period. (4) The glacier runoff in the six representative rivers showed an increasing trend. The contribution rate of glacier runoff to river runoff changed significantly after 2000 but differed among rivers. Overall, the larger the glacier area in the source region is, the greater the contribution rate of glacier runoff is, and the more the contribution rate continuously increases or fluctuates; otherwise, the contribution rate keeps declining, which means the runoff peak may have passed and future runoff may decrease.

Keywords: climate change; glacier mass balance; glacier runoff; PyGEM; Tien Shan



Citation: Wang, H.; Xu, C.; Ying, G.; Liu, F.; Long, Y. Variations in Glacier Runoff Contributed by the Increased Negative Mass Balance over the Last Forty Years in the Tien Shan Mountains. *Water* **2022**, *14*, 1006. <https://doi.org/10.3390/w14071006>

Academic Editor: Yves Tramblay

Received: 14 January 2022

Accepted: 21 March 2022

Published: 22 March 2022

Publisher's Note: MDPI stays neutral with regard to jurisdictional claims in published maps and institutional affiliations.



Copyright: © 2022 by the authors. Licensee MDPI, Basel, Switzerland. This article is an open access article distributed under the terms and conditions of the Creative Commons Attribution (CC BY) license (<https://creativecommons.org/licenses/by/4.0/>).

1. Introduction

Since the 1980s, the climate in Northwest China has experienced a transition from warm-dry to warm-wet [1]. The glacier melting in the Tien Shan Mountains of Central Asia has accelerated due to the increased temperature, leading to changes in runoff components and amount [2–4]. Glaciers, known as “solid reservoirs”, are the headwaters of some major rivers, such as Tarim River, Ili River, Amu Darya, and Syr Darya, in the arid Central Asia and are also one of the critical means of sustaining downstream communities [5–7]. It is of great significance to study the glacier change in the Tien Shan Mountains of Central Asia for sustainable socioeconomic development, the rational allocation and management of water resources, and regional water security in this area.

As the measured mass balance on a large scale is hard to obtain, the energy balance models and degree-day models with the easily collected meteorological elements as input have become important ways to simulate the change in glacier mass and runoff production [8–10]. During the continuous improvement of degree-day models [11–14], many scholars [15–18] began to use ice dynamics to simulate the glacier mass balance and ice thickness, etc. Huss et al. developed the Global Glacier Evolution Model (GloGEM) [16,19] for global glacier change and sea-level rise. Maussion et al. developed the world's first global dynamic glacier simulation model, the Open Global Glacier Model (OGGM) [20], which provides a modular and open-source numerical model framework for simulating past and future changes in any glacier worldwide. Based on the model fame of GloGEM, Rounce et al. [21,22] developed a new Python Glacier Evolution Model (PyGEM). In PyGEM, the spatial variability in mass balance change and runoff predictions can be solved more accurately, and high-precision mass balance geodetic data are used to calibrate the model parameters and quantify the parameter-related uncertainties. Applying the simulation dataset of PyGEM, Shean et al. analyzed the glacier runoff in high-mountain Asia (HMA) and pointed out that the total glacier runoff was $-22.71 \pm 3.01 \text{ Gt yr}^{-1}$ between 2000 and 2018 [23]. Mishra et al. used PyGEM model as glacier hydrology to analyze the economic value of hydropower generation in HMA [24].

While overall the glaciers are retreating in the HMA and long-term glacier monitoring data is available only for a few glaciers in this area, it is difficult to estimate the mass balance for the whole region based on data from the single glacier. At present, research using glacier data that are based on the Randolph Glacier Inventory (RGI) and the second China glacier inventory has become a hotspot globally. In this paper, the geodetic mass balance and glacier runoff data in HMA that were released by Dounce et al. were used to study the glacier change and its climatological and hydrological responses [21]. First, the accuracy of the PyGEM simulated mass balance dataset in the Tien Shan Mountains was evaluated. Then, the change in the glacier mass balance, the glacier's response to climate change, and the variations in glacier runoff contribution rate were analyzed to reveal the impacts of global warming on the Tien Shan glaciers and the associated hydrological processes. The results are expected to provide a scientific basis for regional water resource security as well as the sustainable planning and management of water resources in Central Asia.

2. Data and Methods

2.1. Study Area

The Tien Shan Mountains are located in the arid area of Central Asia, with a latitude from $37^{\circ} 58'$ to $45^{\circ} 79'$ N and a longitude from $66^{\circ} 43'$ to $95^{\circ} 61'$ E. The total length is about 2100 km from east to west and up to 300 km from north to south. Modern glaciers are widely developed. It is one of the mountain systems with the largest distributions of mountain glaciers in the world [25]. As the largest independent zonal mountain system in the world, the Tien Shan Mountains is also the mountain system that is farthest away from an ocean in the world and the largest mountain system in arid areas [26]. It is the source of many rivers in the region and known as “the water tower of Central Asia” [27,28]. The global Randolph Glacier Inventory (RGI 3.2) [29] shows that there are 18,116 glaciers that are distributed in the Tien Shan Mountains, with a total glacial area of approximately $1.42 \times 10^4 \text{ km}^2$, accounting for 28.9% of the total area of glaciers in alpine areas of Asia. Among them, 7934 glaciers are distributed in China, covering an area of 7179 km^2 , and are mainly located in the elevation range of 3800–4800 m [30].

2.2. Data

2.2.1. Glaciological Data

The glacial mass balance data includes measured data and simulation data. (1) The measured data were obtained from the World Glacier Monitoring Service (WGMS, <https://wgms.ch>, accessed on 12 October 2020). They are used to evaluate the accuracy of the simulation data by the PyGEM model. A total of 31 glaciers with measured data that were

available were selected as reference glaciers. Among them, Urumqi River source Glacier No. 1 and Ts. Tuyuksuyskiy glacier have long-term and continuous observations for about 26–34 years. (2) The PyGEM simulation dataset was downloaded from the National Snow and Ice Data Center (<https://nsidc.org/data/highmountainasia>, accessed on 10 May 2021). The original spatial resolution of the simulation data was 0.1° and was resampled to 0.03° when extracting single glaciers. The PyGEM simulation dataset consists of two sets, one is the results that were forced by the European Centre for Medium-Range Weather Forecasts (ECMWF) Reanalysis ERA-Interim data (referred as PyGEM-Interim), and the other is the results that were forced by the Coupled Model Intercomparison Project 5 (CMIP5) simulation data (referred as PyGEM-CMIP5). As the PyGEM-Interim dataset has finer spatial resolution and has been calibrated, it was used for analysis in this study.

The Randolph Glacier Inventory (RGI 6.0) was downloaded from the Global Land Ice Measurements from the Space website (<http://www.glims.org/>, accessed on 23 June 2021). It was used to extract the mass balance data of single glaciers from the PyGEM simulation data. The digital elevation model with a spatial resolution of 30 m was obtained from Geospatial Data Cloud (<http://www.gscloud.cn/>, accessed on 23 June 2021) to delineate the boundary of the Tien Shan Mountains.

2.2.2. Runoff Data

Glacier runoff and its components (including glacier meltwater, glacier precipitation, and glacier snowpack) are from the PyGEM simulation dataset. They are defined following Huss et al. [31]. Glacier runoff (Q) is calculated using liquid precipitation (P_{liquid}), ablation (a), and refreezing (R) as Equation (1), representing the total runoff that is draining out from the initial glacierized area.

$$Q = P_{liquid} + a - R \quad (1)$$

The amount of glacier meltwater is the total amount of glacier ice that melts throughout the accumulation, melting, and refreezing processes. Glacier precipitation, as the precipitation fraction that cannot participate in glacial ice formation, is the sum of liquid precipitation that falls on glacier areas. The glacier snowpack in the ablation area is the amount of snow that is present in the ice-free area that is comprised of the initial glacier area following glacial retreat. This variable represents the regional snow remaining after the accumulation, melting, and re-freezing processes. In the absence of solid precipitation data in regional glacier areas, this paper uses the variables that are listed above (glacier snowpack) to characterize the snowmelt amounts at the glacier terminus.

The measured river surface runoff data are from 6 representative rivers (Figure 1) on the northern and southern slopes of the Tien Shan Mountains. The rivers include the Urumqi River (Hero Bridge Hydrological Station), Manas River (Kenswat Hydrological Station), Toxkan River (Shaliguilank Hydrological Station), Kumarak River (Xiehela Hydrological Station), Kaidu River (Dashankou Hydrological Station), and Weigan River (Heizi Reservoir Station). The measured runoff data were obtained from the Hydrology and Water Resources Bureau of Xinjiang Uygur Autonomous Region and the National Tibetan Plateau Third Pole Environment Data Center (<http://data.tpdc.ac.cn/en/>, accessed on 26 May 2021). They are mainly used for the calculation of the contribution rate of glacier runoff to river runoff.

2.2.3. Meteorological Data

The 2-m monthly temperature and precipitation ERA5 reanalysis data that was released by the European data-forecasting center (ECMWF, <https://www.ecmwf.int/>, accessed on 17 May 2021) from 1980 to 2017 were used in this study. The original spatial resolution of data was 0.25° and was resampled to 0.1° , employing the bilinear interpolation method under ArcGIS to match the glacier mass balance data with the resolution of 0.1° . The data were used to analyze the change in temperature and precipitation in the glacier areas and the response of mass balance to climate change.

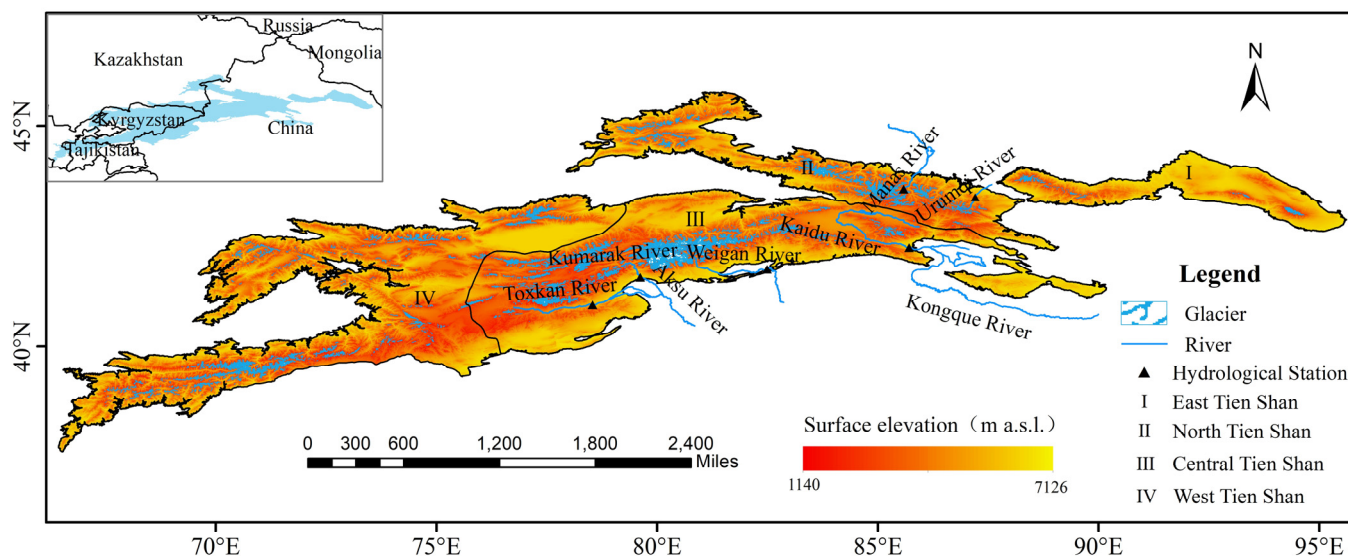


Figure 1. Geographical location map of the Tien Shan Mountains in Central Asia. The inset shows the location of the Tien Shan Mountains. The glacier outlines are from RGI (6.0) and the elevation was based on The Shuttle Radar Topography Mission (SRTM).

2.3. Statistical and Trend Analysis

The spatial correlation analysis [32] was used to analyze the correlations between the temperature, precipitation, and glacier mass balance in the Tien Shan Mountains. The Pearson correlation coefficient represents the correlation degree between the data.

The Mann–Kendall (M-K) test, a nonparametric statistical test method, is often used to test the significance or mutability of long-term trends in time series. In this study, the M-K method was used to analyze the overall change trends of glacier runoff, temperature, and precipitation time series. The specific calculation of the method can be found in the reference by Hamed et al. [33].

3. Results and Analysis

3.1. Accuracy Evaluation of the PyGEM Simulation Data

A total of 31 reference glaciers in the Tien Shan Mountains of Central Asia were used to evaluate the accuracy of the PyGEM simulated data. From the verification results of the 31 glaciers (Figure 2c), the overall correlation coefficient (r) between the measured glacier mass balance data and the PyGEM-Interim data was 0.40, the root-mean-square-error (RMSE) is 0.51, and the mean absolute error (MAE) was 0.41. The PyGEM-Interim simulation data was in good agreement with the measurements, which is consistent with the study by Rounce et al. [21].

The details and the correlation coefficients of the 17 reference glaciers which have continuous and the relatively longer observed data are shown in Table 1. It can be found that the longer the monitoring data, the higher the accuracy of the simulation is. For example, the east and west branches of the Urumqi River source Glacier No. 1, the Ts.Tuyuksuyskiy glacier and the Zoya Kosmodemyanskaya glacier (Table 1, Figure 2a,b) had higher correlation coefficients ranging from 0.55–0.76 ($p < 0.01$). For those glaciers with a short-term monitoring value or small area, the simulation effect was not very good. In general, the PyGEM-Interim simulation data can well capture the inter-annual changes in the glacier mass balance and effectively reflect the change in the mass balance of single glaciers in the study area.

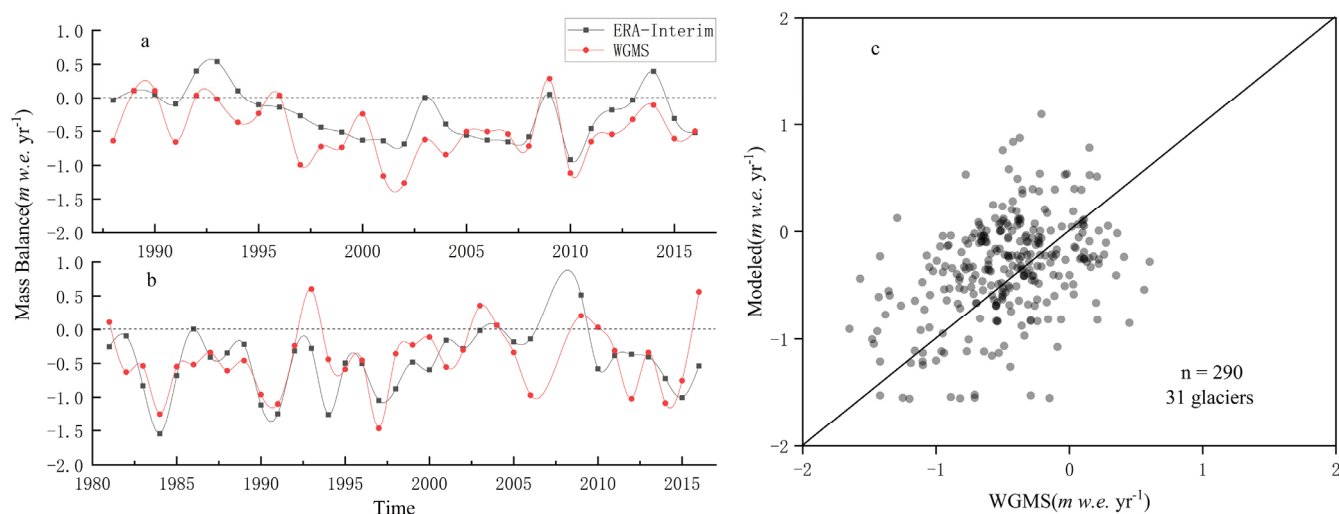


Figure 2. Accuracy evaluation of the PyGEM simulated data. Comparison of the average annual mass balance between the PyGEM-Interim simulated data and WGMS observed data. (a) Urumqi Glacier No. 1 E-Branch during 1988–2016, (b) Ts. Tuyuksuyskiy during 1981–2016, and (c) all the 31 glaciers.

Table 1. Details of the 17 reference glaciers and the correlation coefficients between the PyGEM-Interim glacier mass balance simulated data and the WGMS measured data in the Tien Shan Mountains of Central Asia.

No.	Reference Glacier	Latitude	Longitude	Data Duration (Years)	Correlation Coefficient (r)
1	Urumqi Glacier No. 1 E-Branch	43.111° N	86.811° E	26	0.76 **
2	Urumqi Glacier No. 1 W-Branch	43.118° N	86.804° E	29	0.70 **
3	Golubin	42.46° N	74.495° E	21	0.29
4	Batysh Sook/Syek Zapadny	41.79° N	77.75° E	10	0.64 *
5	Muravlev	45.0954° N	80.2389° E	12	0.63 *
6	Shumskiy	45.08° N	80.23° E	12	0.47
7	Sary Tor (No. 356)	41.83° N	78.174° E	7	0.63
8	Visyachiy-1-2	43.04° N	77.08° E	11	0.65 *
9	Partizan	43.03° N	77.08° E	11	0.72 *
10	Mayakovskiy	43.02° N	77.11° E	11	0.68 *
11	Ordzhonikidze	43.0621° N	77.1031° E	11	0.70 *
12	Zoya Kosmodemyanskaya	43.0507° N	77.0712° E	11	0.75 **
13	Manshuk Mametova	43.0757° N	77.1083° E	11	0.02
14	Molodezhniy	43.056° N	77.0619° E	11	0.67 *
15	Kara-Batkak	42.14° N	78.27° E	22	0.26
16	IGLI Tuyuksu	43.0525° N	77.0986° E	11	0.75 **
17	Ts. Tuyuksuyskiy	43.05° N	77.08° E	34	0.55 **
17	Akshiyek Glacier (No. 354)	41.799° N	78.1506° E	6	0.61

Note: * indicates $p < 0.05$; ** indicates $p < 0.01$.

3.2. Changes in Glacier Mass Balance

3.2.1. Spatial-Temporal Variations in the Glacier Mass Balance

Spatially, obvious regional differences existed in the mass balance changes for the studied glaciers in the Tien Shan Mountains (Figure 3 top). The decreasing rate of the mass balance in the northern West Tien Shan Mountains was the largest (-0.025 m w.e. yr^{-1}), followed by East Tien Shan Mountains, eastern North Tien Shan Mountains, and central West Tien Shan Mountains (-0.022 m w.e. yr^{-1} , -0.019 m w.e. yr^{-1} , and -0.021 m w.e. yr^{-1} , respectively), and that in the Central Tien Shan Mountains was the least (-0.007 m w.e. yr^{-1}).

In contrast, the glaciers in western North Tien Shan, northern West Tien Shan, and southwestern West Tien Shan showed a slow increasing trend in the mass balance, which is consistent with previous studies [34–36]. Overall, the glacier mass balance in the Tien Shan Mountains in Central Asia have been in a massive losing state over the past 40 years.

In terms of temporal change, the overall change in the glacier mass balance in the Tien Shan Mountains (Figure 3h) showed a downward trend since 1980, with a decreasing rate of -0.012 m w.e. yr^{-1} . Throughout the whole study period, 1980–2000 represented a stage of accelerated decline, with a rate of -0.029 m w.e. yr^{-1} ; the average annual mass balance ranged from -0.903 to 0.088 m w.e. yr^{-1} in this period, and the annual average was -0.404 m w.e. yr^{-1} . The negative state of the glacier mass balance has deepened over the years. From 2001 to 2016, the regional mass balance still showed a downward trend, but the declining rate has slowed down (-0.009 m w.e. yr^{-1}). Undeniably, the glaciers are still in a negative balance.

From the perspective of sub-regions, both positive and negative growth trends exist, and there are significant differences in the different periods. From 1980 to 2000, almost all the subregions showed a decreasing trend in the mass balance. From 2000 to 2009, a significant upward trend occurred, with the increasing rate ranging from 0.018 m w.e. yr^{-1} to 0.087 m w.e. yr^{-1} . After 2009, all the subregions showed a decreasing trend again. Thus, over the whole study period, glaciers in East Tien Shan (Figure 3a), central and eastern North Tien Shan (Figure 3b), central West Tien Shan (Figure 3e), and Central Tien Shan (Figure 3g) appeared as an increasingly negative trend, and that in western North Tien Shan (Figure 3c), northeast West Tien Shan (Figure 3d), and southwestern West Tien Shan (Figure 3f) indicated a slightly increasing trend.

3.2.2. Analysis of Factors Affecting the Glacier Mass Balance

In the context of global warming, factors such as temperature and precipitation that determine the formation, development, and evolution of glaciers have changed to varying degrees in the Tien Shan Mountains. As shown in Figure 4a, the temperature in the study region generally showed an upward trend, with zonal distribution characteristics. The warming rate of 0.1 – 0.2 $^{\circ}\text{C}/10$ years, 0.2 – 0.3 $^{\circ}\text{C}/10$ years, 0.3 – 0.4 $^{\circ}\text{C}/10$ years, and 0.4 – 0.5 $^{\circ}\text{C}/10$ years, accounted for 32.15%, 32.18%, 29.5%, and 6.17% of the total area, respectively. Spatially, the temperature increased least in the Central Tien Shan Mountains, while that in the East and West Tien Shan Mountains showed symmetrical increasing distributions. At the same time, the temperature in the North Tien Shan Mountains also showed an increasing trend from west to east. The high value areas of temperature increase were concentrated in regions with elevations that were less than 4000 m. The increasing trends were the most significant in the eastern North Tien Shan Mountains (0.39 $^{\circ}\text{C}/10$ years) and the upper reaches of Kaidu River (0.34 $^{\circ}\text{C}/10$ years). The average annual temperature in the East Tien Shan Mountains was -0.42 $^{\circ}\text{C}$, increasing at a rate of 0.27 $^{\circ}\text{C}/10$ years.

The precipitation is affected by the regional topography and water vapor source in the Tien Shan Mountains, the high-value areas are mainly distributed in Kyrgyzstan, Tajikistan, and the Ili River basin in China. Over the last 40 years, precipitation in the study area has changed with varying degrees (Figure 4b). The eastern Central Tien Shan Mountains and northern West Tien Shan Mountains have mainly experienced an increase in precipitation, while the southwestern West Tien Shan Mountains, central North Tien Shan Mountains and western Central Tien Shan Mountains have mainly experienced a decrease in precipitation. For example, the precipitation change trends in the upper reaches of the Kumarak River and Ili River were -0.17 mm/10 years and -0.31 mm/10 years, respectively.

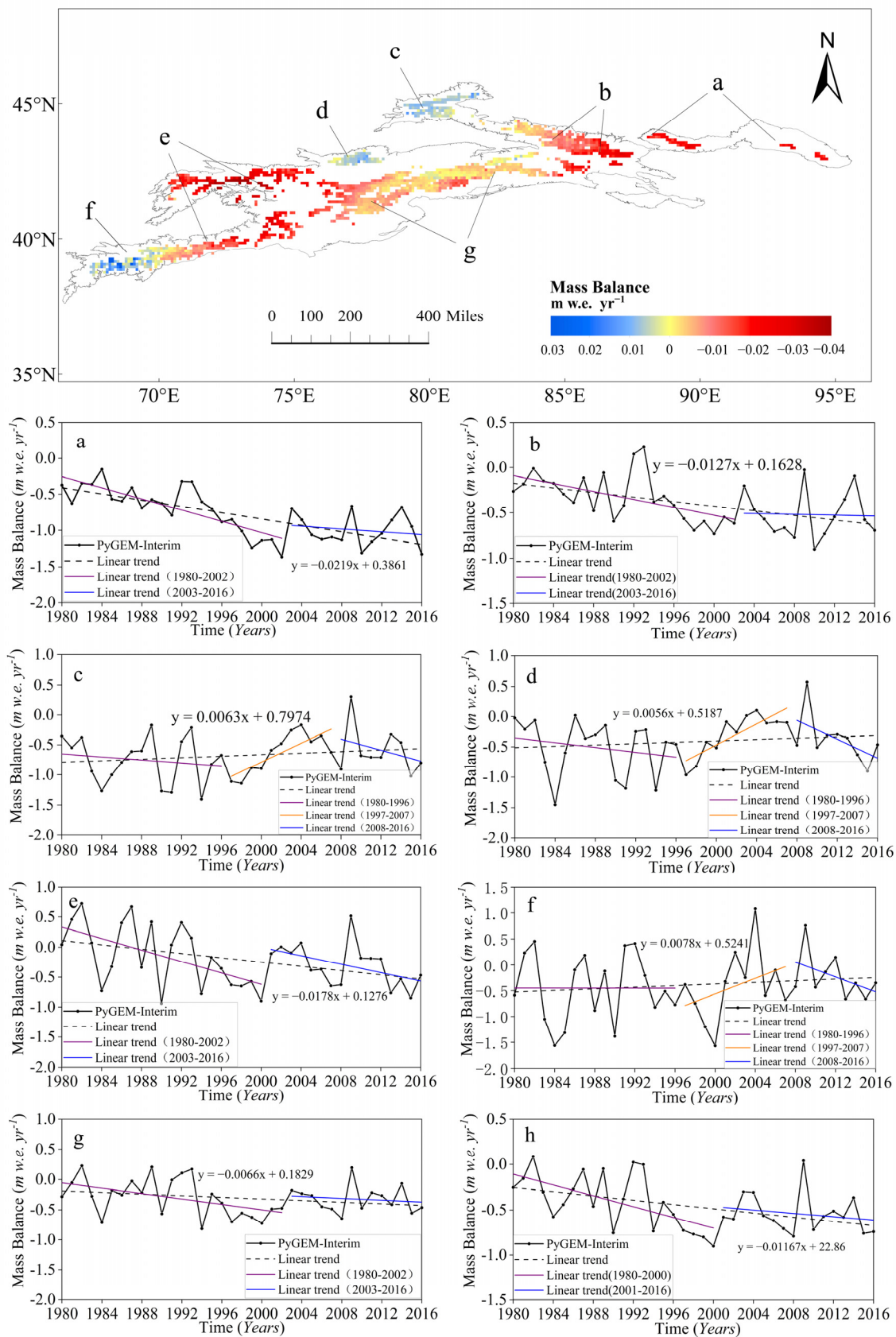


Figure 3. Spatial distribution (top panel) and temporal variations (a–h) in the mass balance of Tien Shan glaciers from 1980 to 2016. (a) East Tien Shan; (b,c) central and eastern, western in North Tien Shan; (d–f) northeast, central, southwest in West Tien Shan; (g) Central Tien Shan; and (h) total.

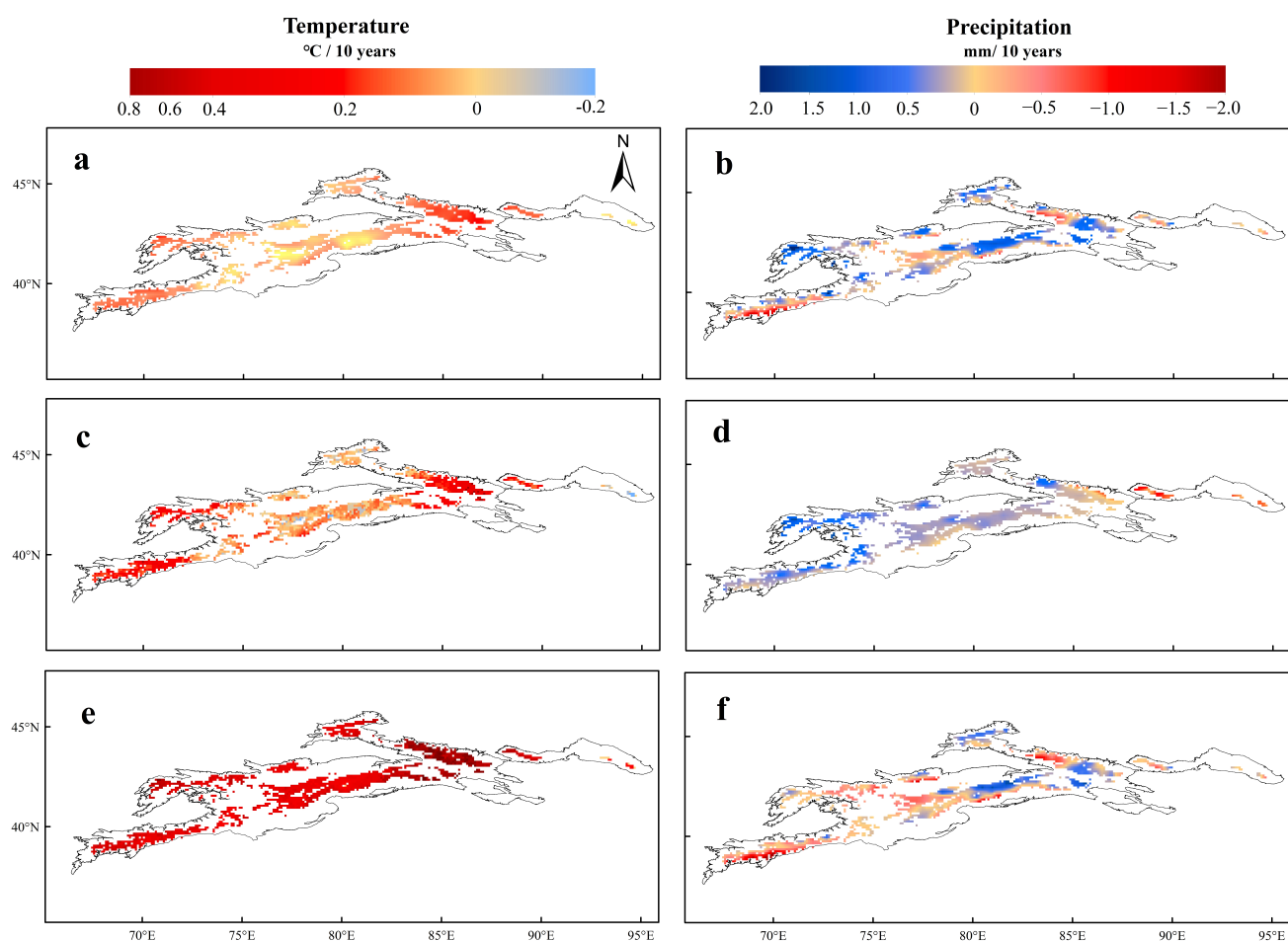


Figure 4. Variations in the linear trend of temperature and precipitation for annual average (a,b), the accumulation period from October to March (c,d), and the ablation period from April to September (e,f) in the Tien Shan Mountains.

The solid precipitation and summer temperature are the critical elements that determine the mass balance of glaciers during the accumulation period (October to March) and the ablation period (April to September), respectively. The changes in temperature and precipitation in the accumulation period and ablation period during the period 1980–2016 were analyzed in this study. The results show that during the accumulation period, the temperature increased most significantly in the central and eastern parts of the North Tien Shan Mountains with the highest increasing rate $0.47\text{ }^{\circ}\text{C}/10\text{ years}$, followed by the upper reaches of the Kaidu River ($0.21\text{ }^{\circ}\text{C}/10\text{ years}$) and the southern Tien Shan Mountains ($0.2\text{ }^{\circ}\text{C}/10\text{ years}$). The warming rate in the East Tien Shan Mountains was relatively low, at only $0.12\text{ }^{\circ}\text{C}/10\text{ years}$, with the western part significantly higher than the eastern part (Figure 4c). The precipitation showed an increasing trend during the accumulation period and increased significantly in the West Tien Shan Mountains, with a maximum increase rate of $1.26\text{ mm}/10\text{ years}$ (Figure 4d). In contrast, the precipitation showed weak decreasing trends in the East Tien Shan Mountains and the eastern North Tien Shan Mountains. During the ablation period, the temperature showed a significant increasing trend in the whole glacier area of the Tien Shan Mountains. In the central and eastern North Tien Shan Mountains, the eastern Central Tien Shan Mountains and the East Tien Shan Mountains, the warming rates were as high as $0.61\text{ }^{\circ}\text{C}/10\text{ years}$, $0.47\text{ }^{\circ}\text{C}/10\text{ years}$, and $0.19\text{ }^{\circ}\text{C}/10\text{ years}$, respectively. The low increasing rates were mainly concentrated in the high-elevation areas of the Central Tien Shan Mountains, such as the Tomor Peak and the Khan Tengri Peak. The precipitation in the Tien Shan glacier area changed steadily overall but spatially different during the ablation period, showing a significant increase in the western and eastern North

Tien Shan Mountains and the eastern and northern Central Tien Shan; the proportion of the area where the precipitation increased was 44.8%. In comparison, the rapid rising temperature is still the main factor affecting the glacier mass balance in the study area.

3.2.3. Response of Glacier Mass Balance to Temperature and Precipitation

Obvious spatial differences can be found in the response of glaciers due to climate change in the Tien Shan Mountains. Figure 5a shows that the correlation between the temperature and mass balance during the accumulation period from 1980 to 2016 is mainly positive in the Tien Shan glacier area; the areas with positive correlations accounted for 75.9% of the total area, and 68% of them have a correlation coefficient between 0.6 and 1. Only approximately 24.1% of the study area showed a negative correlation, which were mainly distributed in the northwestern and southwestern West Tien Shan Mountains and the eastern East Tien Shan Mountains.

During the ablation period, a negative correlation was found between the temperature and mass balance change in the Tien Shan glacier area as a whole (Figure 5c). The correlation coefficient ranged between -0.45 and -1 , with a regional average of -0.71 ; the negative correlations are most significant in the West Tien Shan Mountains (Table 2). On the whole, although the temperature was highly positively correlated with the glacier mass balance change during the accumulation period in the North Tien Shan Mountains and the Central Tien Shan Mountains, the impact of temperature on the glacier mass balance change in the Tien Shan Mountains was dominated by negative correlations during the ablation period. The warming trend of temperature during the ablation period accelerates the melting of regional glaciers.

Table 2. Pearson correlation coefficient between the temperature/precipitation and the mass balance in the subregions.

	Temperature		Precipitation	
	Accumulation Period	Ablation Period	Accumulation Period	Ablation Period
North Tien Shan	0.6 *	-0.68 *	0.81 **	-0.47 **
Central Tien Shan	0.68 *	-0.66 *	0.82 **	-0.45 **
West Tien Shan	-0.11 *	-0.79 *	0.65 **	-0.04 **
East Tien Shan	0.1 *	-0.7 *	0.36 **	-0.56 **

Note: * indicates $p < 0.05$; ** indicates $p < 0.01$.

As shown in Figure 5b, during the accumulation period, the precipitation was mainly positively correlated with the change in the glacier mass balance, which confirms the result that the area with positive snow storage trend usually corresponds to the regions with positive mass balances [37]. The area with correlation coefficients in a range of 0–0.75 and 0.75–1 accounted for 38% and 61% of the whole glacier area, respectively; only a small portion (1%) of the whole area showed a weak negative correlation. As indicated by the correlation distribution (Table 2), the glacier mass balance of the North Tien Shan Mountains and Central Tien Shan Mountains was most obviously affected by precipitation during the accumulation period. The increased precipitation during the glacier mass accumulation process is conducive to glacier development.

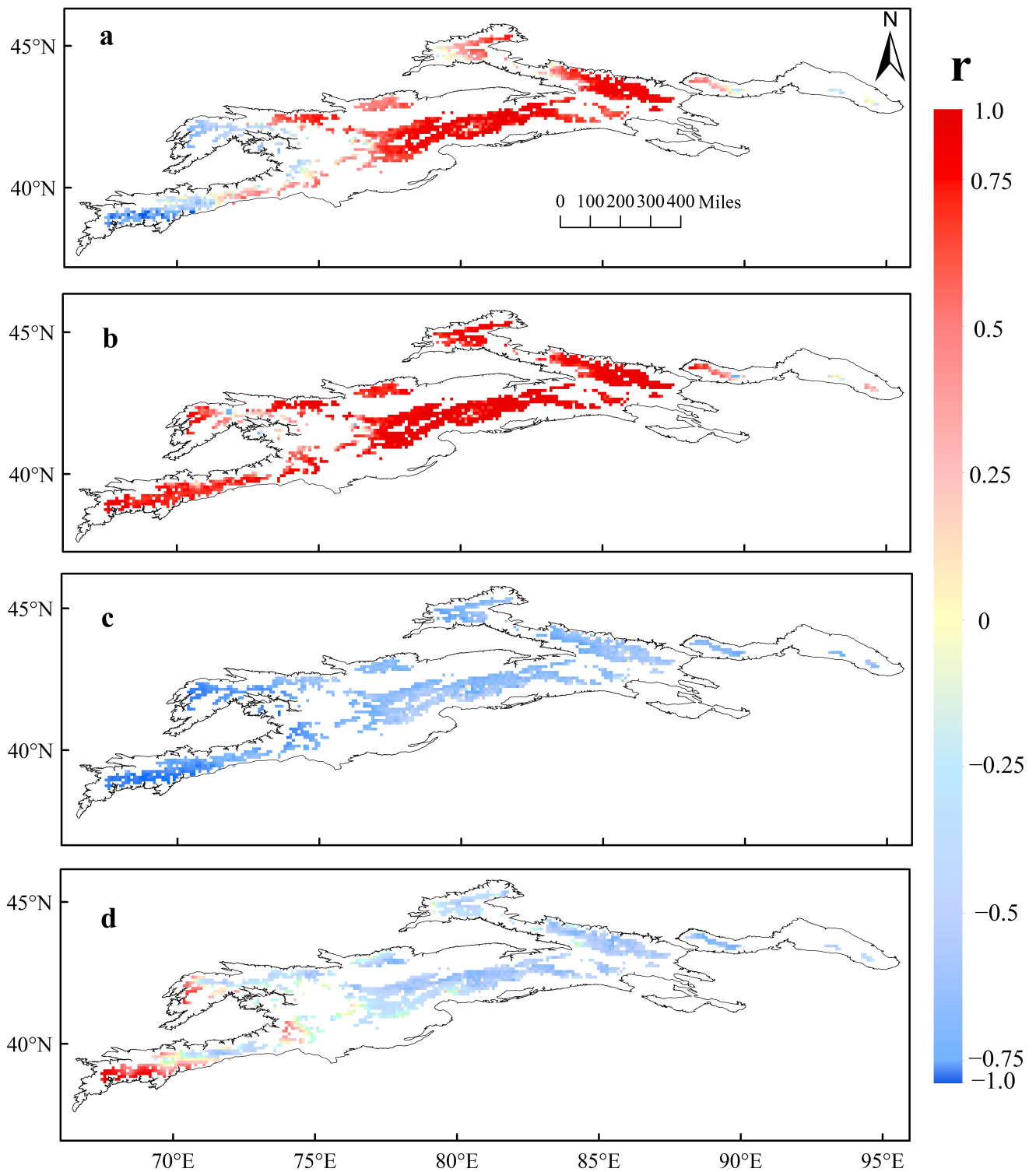


Figure 5. Spatial correlations between the mass balance change and temperature in the accumulation period (a), precipitation in the accumulation period (b), temperature in the ablation period (c), and precipitation in the ablation period (d).

During the ablation period, the precipitation was generally negatively correlated with the change in the glacier mass balance (Figure 5d), and the regional mean correlation coefficient is -0.31 ; the most significant negative correlation was found in the East Tien Shan Mountains, with a regional correlation coefficient (-0.56) much higher than those that were found in the other subregions. While in some areas (only 15.5%), the precipitation was positively correlated with the change in the glacier mass balance, concentrating in the high-elevation regions such as Tomur Peak in the Central Tien Shan Mountains and the western West Tien Shan Mountains.

3.3. Changes in Glacier Runoff

3.3.1. Interannual Variations in Glacier Runoff

Glacier runoff plays an important role in regional water resource allocation and management. Figure 6a shows the spatial distribution of variation trend of glacier runoff from 1980 to 2016 in the Tien Shan glacier area. The areas with increasing trends accounted for 94.85% of the whole glacier area. Especially, the increase was more obvious in southwest West Tien Shan and North Tien Shan Mountains, with the maximum rate reaching $0.1714 \times 10^7 \text{ m}^3/\text{year}$; only a small portion (5.15%) showed a decreasing trend, which were mainly distributed in Central Tien Shan. Combined with the spatial correlation analysis and the temporal variations in glacier runoff and impact factors (Figure 6b–d,f), glacier runoff has a positive correlation with regional precipitation, while regional glacier area and temperature have a more significant impact on glacier runoff. In the central and eastern parts of the Northern Tien Shan Mountains, where glacier runoff is significantly negatively correlated with glacier area, the glacier area is shrinking accompanied by the increased glacier runoff. However, in the southwest of West Tien Shan, the glacier runoff was positively correlated with the area, and negatively correlated with temperature overall, which is consistent with the change of regional mass balance. This also reflects that the increasing trend of temperature is at a lower level in the accumulation period, which not only contributes to the accumulation of regional glacier mass balance, but also helps the increase of glacier runoff.

The change of glacier runoff in the Tien Shan Mountains from 1980 to 2016 (Figure 6e) shows that the glacier runoff, glacier meltwater, and glacier precipitation in the glacier areas all showed an increasing trend, while the glacier snowpack in glacier areas showed a decreasing trend. Among these variables, glacier runoff has increased by 46.34% from 16.077 billion m^3 in 1980 to 23.526 billion m^3 in 2000. From 2001 to 2016, the glacier runoff increased significantly weaker than the previous period. The M-K trend test also indicates that the glacier runoff increased and maintained a relatively stable and highly oscillating state. The change in glacial meltwater is consistent with that of the total glacier runoff, displaying an overall increase and large interannual fluctuations. The glacier snowpack, which is affected by the increasing temperature and decreasing solid precipitation, decreased by 11.69% over that in the 1980s, while the liquid precipitation (glacier precipitation) in the glacier areas increased by 19.39%. With respect to glacier shrinkage, the glacier area shrinks, and the amount of snow originally belonging to the glacier area thus also decreases [38,39]. This also indicates that the decrease in the glacier mass balance is not only caused by rising temperature but is also exacerbated by the decrease of solid precipitation that is recharged at glacier terminals and lower altitudes.

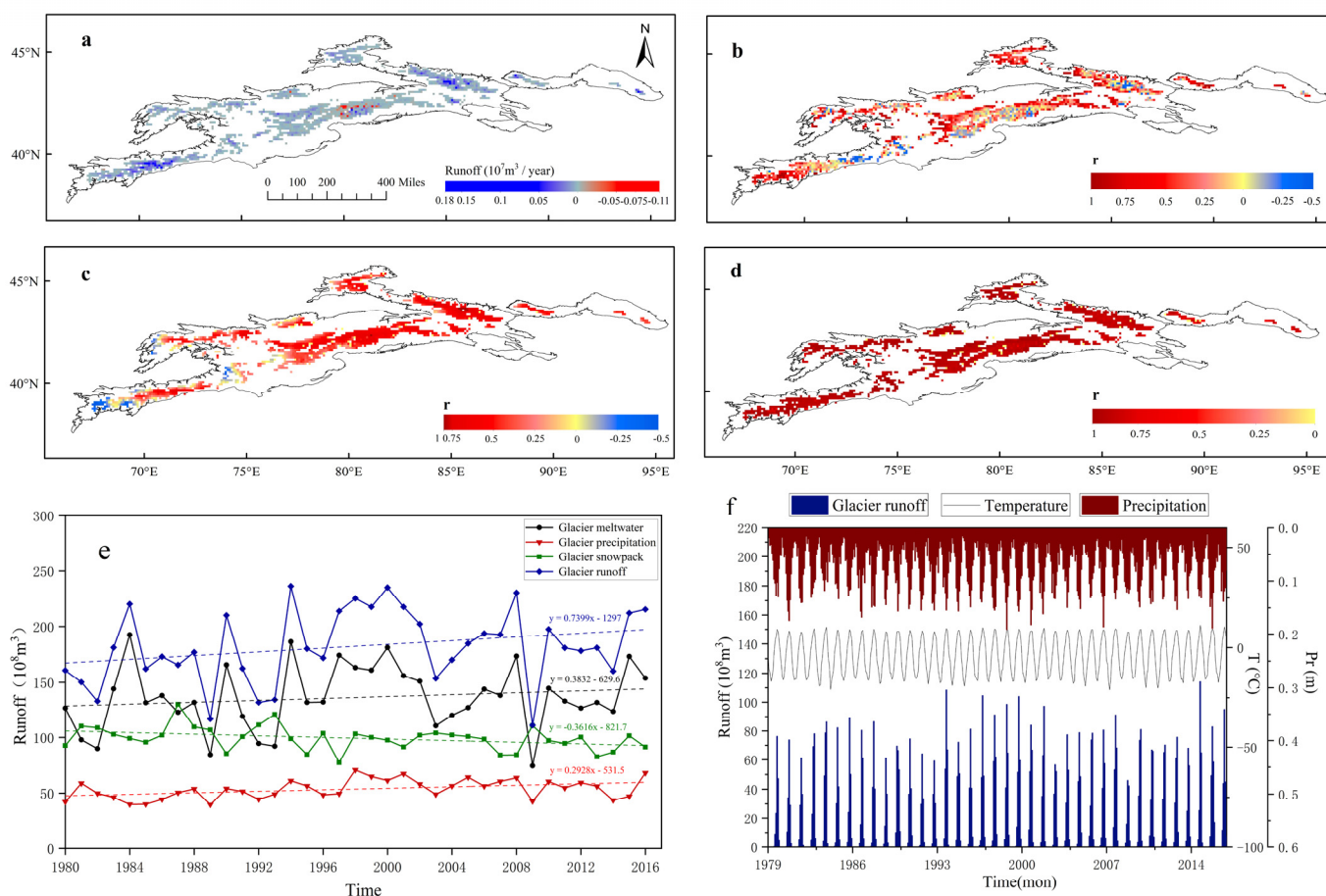


Figure 6. Change in glacier runoff and impact factors in the Tien Shan Mountains from 1980 to 2016. Spatial distribution (a) and temporal variations (e) of glacier runoff; spatial correlations between glacier runoff and glacier area (b), temperature (c), and precipitation (d) from 1980 to 2016; The monthly temporal variation trend of glacier runoff and influencing factors (f).

3.3.2. Intra-Annual and Interdecadal Variations in Glacier Runoff

The distribution of glacier runoff is uneven throughout the year due to the influence of continental climate. It is concentrated from May to September each year and reaches a peak in July (Figure 7a). The intra-annual distribution of glacier meltwater is consistent with that of glacier runoff (Figure 7b). The glacier snowpack in the ablation area displays a “double-peak” phenomenon throughout the year, with a higher peak in May and a lower peak in September. The glacier precipitation (liquid precipitation) is mostly concentrated from June to August owing to the higher summertime temperatures.

From the interdecadal point of view, the glacier meltwater that was measured in July began to rise from the 1980s and reached peak in the 1990s. At the same time, the glacier meltwater that was measured in August has been increasing since the 21st century, and the peak period has been prolonged. The glacier precipitation has also maintained increasing trends since the 1980s (Figure 7c). In July, when the most liquid precipitation falls, the precipitation increased by nearly 24.36% from the 1980s to the 2000s. Since the 1980s, the glacier snowpack in the ablation area has continuously decreased (Figure 7d). The snowpack in May in the early 2000s and 2010s has decreased by 11.84% and 10.65% over that in the 1980s, respectively. The snowpack in September, however, exhibited interdecadal fluctuations and reached a maximum in the 2000s.

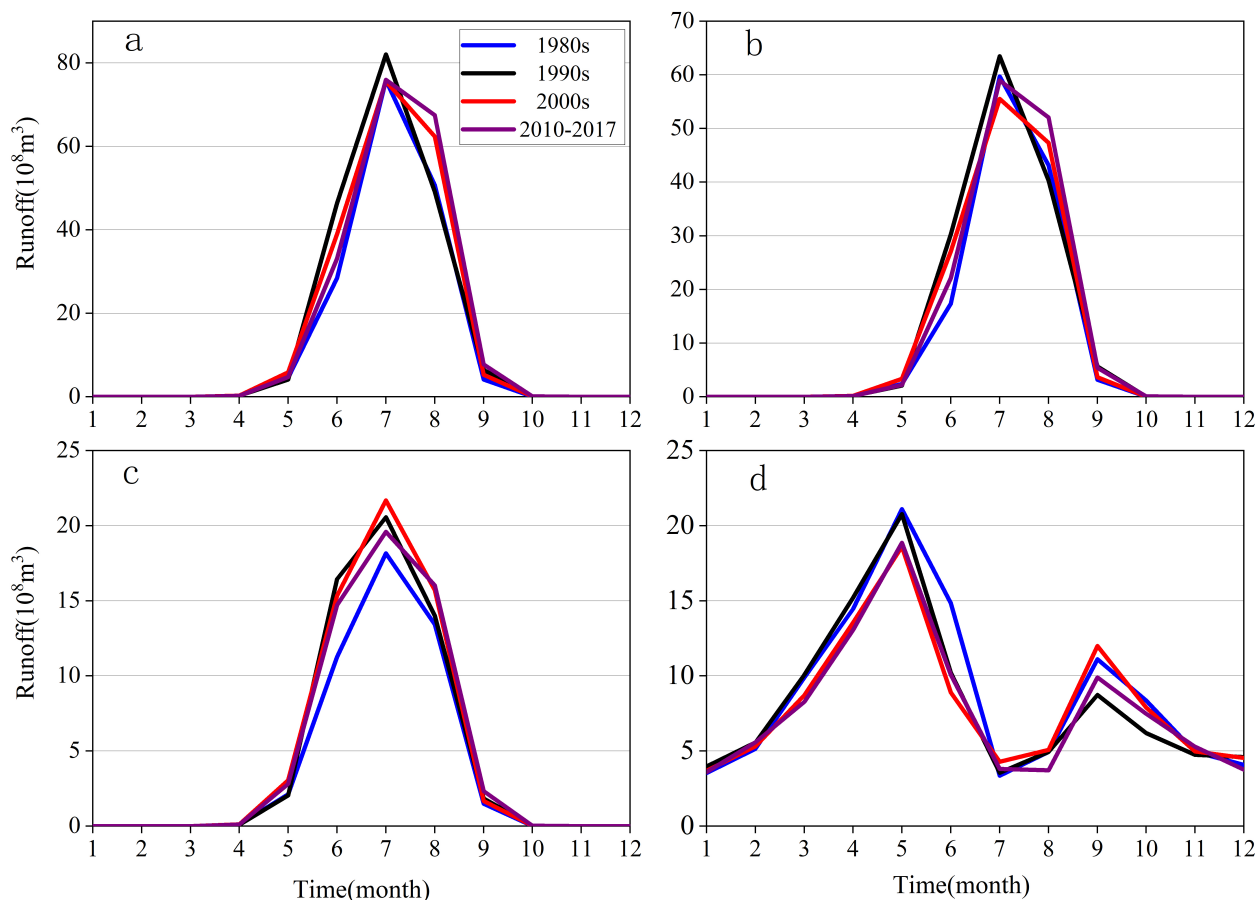


Figure 7. Intra-annual and interdecadal variations in glacier runoff (a) and its components ((b) glacier meltwater, (c) glacier precipitation, and (d) snowpack) in the Tien Shan Mountains of Central Asia from 1980 to 2016.

The intra-annual and interdecadal changes that were recorded in the glacier runoff show that the maximum melting time of the glaciers had not changed in July; however, an obvious increasing trend in glacier melt was observed in August. Under the joint action of the higher melting rates and the increased liquid precipitation during August, the glacier runoff also increased, and the solid precipitation decreased. This finding is consistent with the previous research by Deng et al. [40].

3.3.3. Inter-Annual Variations in Glacier Runoff

Taking the six rivers that are distributed on the northern and southern slopes of the Tien Shan Mountains as the representative rivers, the inter-annual variations in glacier runoff was investigated. Similarities and differences both can be found among the watersheds (Figure 8). The similarity is that the glacier runoff in all six rivers showed an obvious increasing trend before 2002. Among them, the increased rate of glacier runoff in the Kumarak River was the highest, reaching $2.45 \times 10^8 \text{ m}^3/10\text{a}$, and that of Urumqi River was the lowest, at only $0.87 \times 10^8 \text{ m}^3/10\text{a}$. After 2002, however, the increasing rates of glacier runoff in some rivers decelerated or showed downward trends. For example, the glacier runoff in the Kaidu River and Urumqi River showed an obvious downward trend, with the increasing rate of $-1.033 \times 10^8 \text{ m}^3/10\text{a}$ and $-0.075 \times 10^8 \text{ m}^3/10\text{a}$, respectively. The glacier runoffs that were measured in Tuoxkan River and Weigan River were relatively stable, showing weak downward trends. In the Kumarak River and Manas River, glacier runoff still showed increasing trends, but the increase rates were significantly lower than those that were measured before 2000. In general, the glacier runoff that was measured in watersheds with higher glacier proportions generally still showed upward trends, but

in watersheds with lower glacier proportions, the glacier runoff displayed non-significant increasing trends or even obvious downward trends.

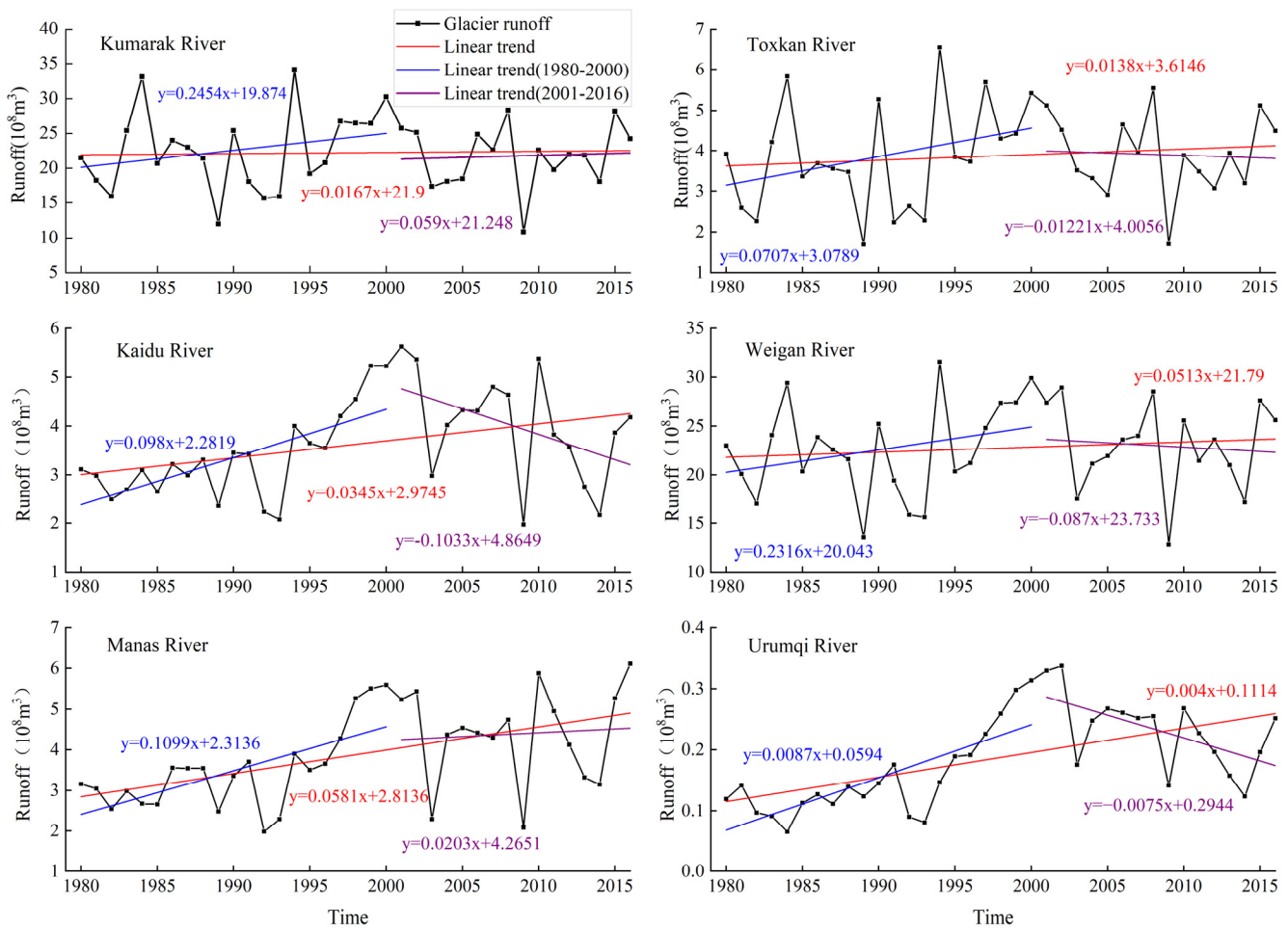


Figure 8. Inter-annual variations in glacier runoff in six watersheds.

3.4. Variations in the Contribution of Glacier Runoff to River Runoff

With respect to the overall retreat of regional glaciers, the increase in glacier melt is one of the main causes of the observed continuous increase in runoff in the rivers in the Tien Shan Mountains [41]. Changes in the contribution rates of glacier runoff to river runoff in the six representative rivers (Table 3) indicate that the increased glacier melting rates have been observed in the rivers that are fed mainly by glacier meltwater, such as the Kumarak River, Weigan River, and Manas River, and glacier runoff has maintained a high supply capacity to the river runoff since 2000. For the rivers that are fed less by glacier meltwater, such as the Kaidu River, Urumqi River, and Toxkan River, the contribution rates showed a certain decreasing trend.

Table 3. Details of the six representative rivers and variations in the contribution of glacier runoff to river runoff in the Tien Shan Mountains of Central Asia.

	River Source Area (km ²)	Proportion of Glacier Area (%)	Average Annual River Runoff (10 ⁸ m ³)	Average Annual Glacier Runoff (10 ⁸ m ³)	Reference (1980–2007)	Contribution Rate (%)				
						1980–1999	2000–2005	2006–2010	2011–2016	Annual
Kumarak River	14,064.23	18.07	49.85	22.25	52.43–58.65 [5,42–44]	45.44	42.63	43.22	48.22	44.38
Toxkan River	10,893.18	5.11	31.21	3.99	26.1–29.2 [42,45]	13.85	11.80	14.07	14.30	13.62
Kaidu River	20,908.44	1.71	38.86	4.12	21.1–33.80 [45]	9.82	11.25	10.56	10.21	10.03
Weigan River	18,489.12	9.32	29.71	23.40	71 [46]	83.36	81.79	78.18	76.39	81.28
Manas River	5817.83	9.14	14.31	3.92	19–34.6 [5,47]	26.86	31.63	30.02	30.78	28.70
Urumqi River	1061.17	2.55	2.40	0.24	11.3 [48]	5.74	12.14	10.27	7.90	7.74

In terms of specific watersheds, the contribution rates of glacier runoff to river runoff in the Toxkan River and Kumarak River, the two major tributaries of the Aksu River Basin, were different, with 13.88% and 47.16%, respectively; these values increased by 0.9% and 4.06%, respectively, compared with that in the 2000s. The number of glaciers in the Kaidu River basin is small, with the annual average contribution rate only 10.03%, from 2000 to 2016, the contribution proportion continuously decreased and reached the lowest value in 2010 (4.67%). The supply of glacier runoff to river runoff in the Kaidu River basin is weakening annually, which is also shown in the research by Duan et al. [49]. The contribution rate in the Weigan River basin is much higher than those that were measured in other rivers, with an average of approximately 80%; however, this rate has also shown a decreasing trend since 2000 from 81.79% in 2000–2005 to 76.39% in 2011–2016. The contribution rates in the Manas River and Urumqi River, both originated from the North Tien Shan Mountains, decreased after 2000. The contribution rate in the Urumqi River decreased significantly from 11.29% in the 2000s to 7.9% in 2011–2016. However, the contribution rate in the Manas River showed a weak and relatively gentle downward trend fluctuating between 30% and 35%.

4. Discussion

4.1. Impact of Climate Change on the Glacier Mass Balance

Temperature controls the glacier-melting process while solid precipitation determines the glacier accumulation [30]. The mass balance was the mass basis for the changes of glacier runoff. In the context of global warming, the spatial differentiation of glacier mass balance changes in the Tien Shan Mountains is obvious due to the continental climate conditions and various geographical locations. By comparing the mass balance changes that were observed in typical glaciers in different regions of the Tien Shan Mountains, Wang et al. [50] reported that the observed changes in glaciers in the region were affected by the westerly winds and that the differences in water and heat combinations in the region formed the continuous reductions that were observed in the mass balance distribution of glaciers from west to east. Farinotti et al. [51] used Gravity Recovery and Climate Experiment (GRACE) satellite data to conclude that the glaciers in the Tien Shan Mountains are affected by global warming and that glacier melting accelerates in summer, thus reducing the annual average mass balance of glaciers in the region by $18 \pm 6\%$ from 1961 to 2012, with a decreasing rate of $-5.4 \pm 2.8 \text{ Gt yr}^{-1}$. To explore the impact of climate change on the mass balance of glaciers in the Tien Shan Mountains, we calculated the correlation coefficients of mass balance with temperature and precipitation, respectively. Combined with the observed changes in glacier mass balance and their response to climate change during the glacier accumulation and melting periods, we found that the negative mass balance of the Tien Shan glaciers is still dominated by the continuous rise in the regional temperature. The rising temperature during the glacier ablation period has the most significant impact on the observed negative mass balance. During the accumulation period, the increasing

temperature reduced the supply of solid precipitation to the glaciers and accelerated the mass loss of the glaciers in the Tien Shan Mountains. The positive mass balances that were measured in some glaciers are mainly due to the decreasing regional temperature during the accumulation period, low rates of temperature increase during the ablation period, and increasing precipitation. The increasing process of mass balance in these glaciers is similar to the glacier surges and positive mass balance phenomenon that is found in the Karakoram Mountains [52]; the occurrence of such changes in regional climate may be related to abnormal fluctuations in South Asian low pressure and Iranian high pressure in recent years [53]. The mechanism of regional climate change and its impacts on glacier mass balance needs to be further studied.

4.2. Change in River Supply under the Increasingly Negative of the Glacier Mass Balance

Changes in the glacier mass balance inevitably lead to fluctuations in glacier runoff in the corresponding regions, and these fluctuations affect the supply mode of river runoff. Most of the rivers in the arid area of Central Asia originate from alpine glacier areas. In the whole study region, the interannual fluctuations in glacier runoff that are caused by changes in the glacier mass balance and changes in the contribution rate of glacier runoff to river runoff are significant. For example, in the Tarim River basin, the largest inland river basin in China, the contribution rate of meltwater to river runoff increased significantly from 41.5% to 46.5% from 1961 to 1990 [54]. In the Turpan-Hami basin, with a small number of glaciers, the contribution rate of glacier runoff to surface runoff was only 11.4% [55], the increase in runoff tended to decelerate after 2000 [56], and the contribution proportion also decreased. On the whole, the amount of glacier runoff feeding to rivers in the Tien Shan Mountains is still greatly affected by the area of glaciers in the source region of each river, and the glacier mass balance in the region is generally in an increasingly negative state. The glacier area and number in the source area determine the abundance and change of glacier runoff; the glacier runoff in watersheds with high glacier area proportions still generally presents an upward trend. Therefore, the contribution rate of glacier runoff to river runoff is also increasing; in watersheds with small glacier area in source region, the increase rate of glacier runoff decelerated or showed a downward trend after 2002. Meanwhile, the contribution rate of glacier runoff to river runoff has continually decreased in some rivers, indicating that the glaciers in these watersheds may have reached the melting peak.

5. Conclusions

The PyGEM-Interim simulation data can effectively reproduce the change trends of the glaciers mass balance in the Tien Shan Mountains during the historical period (1980–2016). The correlation coefficient (r) between PyGEM-Interim simulation data and WGMS measured data was 0.402, and the RMSE was 0.51.

Since 1980, the “deficit” in the glacier mass balance has been increasing, and regional glaciers are still shrinking at a high level. From the end of 1980 to the beginning of 2000, the decadal average mass balance of glaciers in the Tien Shan Mountains changed continuously at a rate of -0.027 m w.e. yr^{-1} ; after 2000, the regional mass balance maintained a high negative balance under an increasingly negative change trend, with the average annual mass balance reaching -0.564 m. w.e. yr^{-1} .

Over the last 40 years, the temperature has shown a significant upward trend during the glacier accumulation period in the study area, and the precipitation has also increased significantly in most regions. Although positive increases in glacier mass balance have been observed in some regions of the West Tien Shan Mountains, the correlation between the temperature and mass balance is much higher than that between the precipitation and mass balance; temperature dominates the development of regional glacier changes.

The changes in the runoff in the Tien Shan Mountains are closely related to changes in the glacier mass balance. Since the 1990s, the “deficit” in the mass balance in the Tien Shan Mountains has not only led to the overall retreat of glaciers in the region but also increased the glacier runoff, and then had great impacts on the regional river runoff with a

varying contribution rate due to the sizes of the glacier areas in the headwaters of different watersheds. In general, the more widely distributed the glaciers in the source area is, the greater the contribution rate of glacier runoff, and the larger supply capacity of the glacier runoff. In contrast, the contribution rates of some glaciers have decreased, and the glacier melt supply of some rivers, such as the Kaidu River and Urumqi River, may have reached the peak and begun to decline.

Author Contributions: H.W. and C.X. contributed to the conception and design of the study, and H.W. wrote the manuscript. G.Y. and F.L. assisted H.W. in statistical analysis of the data. H.W. and Y.L. modified the figures. All authors have read and agreed to the published version of the manuscript.

Funding: This work is supported by the National Natural Science Foundation of China (No. 42067062).

Data Availability Statement: No new data were created or analyzed in this study. Data sharing is not applicable to this article.

Acknowledgments: We are very grateful for the measured data of regional runoff and glacier mass balance that were provided by the Hydrology and Water Resources Bureau of Xinjiang Uygur Autonomous Region, the National Tibetan Plateau Third Pole Environment Data Center and the World Glacier Monitoring Service (WGMS). In addition, We would like to express our heartfelt thanks to David Rounce (Carnegie Mellon University in Pittsburgh, USA), for sharing PyGEM model data and providing help in the process of model data learning and processing.

Conflicts of Interest: The authors declare no conflict of interest.

References

- Shi, Y.F. Preliminary Study on Signal, Impact and Foreground of Climatic Shift from Warm-Dry to Warm-Humid in Northwest China. *J. Glaciology Geocryol.* **2002**, *24*, 219–226. [[CrossRef](#)]
- Yao, T.; Wang, Y.; Liu, S.; Pu, J.; Shen, Y.; Lu, A. Recent glacial retreat in High Asia in China and its impact on water resource in Northwest China. *Sci. China Ser. D Earth Sci.* **2004**, *47*, 1065–1075. [[CrossRef](#)]
- Chen, Y.; Li, Z.; Fang, G.; Deng, H. Impact of Climate Change on Water Resources in the Tianshan Mountains, Central Asia. *Acta Geogr. Sin.* **2017**, *72*, 18–26. [[CrossRef](#)]
- Kuzmichenok, V.; Aizen, V.; Surazakov, A.; Aizen, E. Assessment of Glacial Area and Volume Change in Tien Shan (Central Asia) During the Last 60 Years Using Geodetic, Aerial Photo, Aster and Strm Data. *AGU Fall Meet. Abstr.* **2004**, *69*, 59–70.
- Yang, Z. Glacial Water Resources in China. *Resour. Sci.* **1987**, *1*, 46–55, 68.
- Zemp, M.; Huss, M.; Thibert, E.; Eckert, N.; McNabb, R.; Huber, J.; Barandun, M.; Machguth, H.; Nussbaumer, S.U.; Gärtner-Roer, I.; et al. Author Correction: Global glacier mass changes and their contributions to sea-level rise from 1961 to 2016. *Nature* **2020**, *577*, 382–386. [[CrossRef](#)] [[PubMed](#)]
- Dehecq, A.; Gourmelen, N.; Gardner, A.S.; Brun, F.; Goldberg, D.; Nienow, P.W.; Berthier, E.; Vincent, C.; Wagnon, P.; Trouvé, E. Twenty-first century glacier slowdown driven by mass loss in High Mountain Asia. *Nat. Geosci.* **2019**, *12*, 22–27. [[CrossRef](#)]
- Cazorzi, F.; Fontana, G.D. Snowmelt modelling by combining air temperature and a distributed radiation index. *J. Hydrol.* **1996**, *181*, 169–187. [[CrossRef](#)]
- Hock, R. Temperature index melt modelling in mountain areas. *J. Hydrol.* **2003**, *282*, 104–115. [[CrossRef](#)]
- Kang, S.E.; Ohmura, A. Energy, Water and Mass Balance and Runoff Models in Tianshan Glacier Affected Area. *Chin. Sci. Part B Chem. Life Sci. Geosci.* **1994**, *24*, 983–991.
- Gong, Z.-Z.; Xie, H.-S.; Liu, Y.-G.; Huo, H.; Jing, F.-Q.; Guo, J.; Xu, J.-A. High-Pressure Sound Velocity of Perovskite-Enstatite and Possible Composition of Earth's Lower Mantle. *Chin. Phys. Lett.* **1999**, *16*, 695–697. [[CrossRef](#)]
- Radic, V.; Hock, R. Regionally differentiated contribution of mountain glaciers and ice caps to future sea-level rise. *Nat. Geosci.* **2011**, *4*, 91–94. [[CrossRef](#)]
- Zhang, Y.; Liu, S.; Wang, X. A Dataset of Spatial Distribution of Degree-Day Factors for Glaciers in High Mountain Asia. *Chin. Sci. Data Chin. Engl. Online Ed.* **2019**, *4*, 137–147. [[CrossRef](#)]
- Di Marco, N.; Righetti, M.; Avesani, D.; Zaramella, M.; Notarnicola, C.; Borga, M. Comparison of MODIS and Model-Derived Snow-Covered Areas: Impact of Land Use and Solar Illumination Conditions. *Geosciences* **2020**, *10*, 134. [[CrossRef](#)]
- Huss, M.; Farinotti, D. Distributed ice thickness and volume of all glaciers around the globe. *J. Geophys. Res. Earth Surf.* **2012**, *117*, F04010. [[CrossRef](#)]
- Huss, M.; Hock, R. A New Model for Global Glacier Change and Sea-Level Rise. *Front. Earth Sci.* **2015**, *3*, 503–519. [[CrossRef](#)]
- Kienholz, C.; Rich, J.L.; Arendt, A.A.; Hock, R. A New Method for Deriving Glacier Centerlines Applied to Glaciers in Alaska and Northwest Canada. *Cryosphere* **2014**, *8*, 503–519. [[CrossRef](#)]
- Yao, X.; Liu, S.; Zhu, Y.; Gong, P.; Lina, A.N.; Li, X. Design and Implementation of an Automatic Method for Deriving Glacier Centerlines Based on Gis. *J. Glaciol. Geocryol.* **2015**, *6*, 1563–1570. [[CrossRef](#)]

19. Hock, R.; Bliss, A.; Marzeion, B.; Giesen, R.H.; Hirabayashi, Y.; Huss, M.; Radić, V.; Slangen, A.B.A. GlacierMIP—A model intercomparison of global-scale glacier mass-balance models and projections. *J. Glaciol.* **2019**, *65*, 453–467. [[CrossRef](#)]
20. Maussion, F.; Butenko, A.; Champollion, N.; Dusch, M.; Eis, J.; Fourteau, K.; Gregor, P.; Jarosch, A.H.; Landmann, J.; Oesterle, F.; et al. The Open Global Glacier Model (OGGM) v1.1. *Geosci. Model Dev.* **2019**, *12*, 909–931. [[CrossRef](#)]
21. Rounce, D.R.; Hock, R.; Shean, D.E. Glacier Mass Change in High Mountain Asia Through 2100 Using the Open-Source Python Glacier Evolution Model (PyGEM). *Front. Earth Sci.* **2020**, *7*, 331. [[CrossRef](#)]
22. Rounce, D.R.; Khurana, T.; Short, M.B.; Hock, R.; Shean, D.E.; Brinkerhoff, D.J. Quantifying parameter uncertainty in a large-scale glacier evolution model using Bayesian inference: Application to High Mountain Asia. *J. Glaciol.* **2020**, *66*, 175–187. [[CrossRef](#)]
23. Shean, D.E.; Bhushan, S.; Montesano, P.M.; Rounce, D.R.; Osmanoglu, B. A Systematic, Regional Assessment of High Mountain Asia Glacier Mass Balance. *Front. Earth Sci.* **2020**, *7*, 363. [[CrossRef](#)]
24. Mishra, S.K.; Veselka, T.D.; Prusevich, A.A.; Grogan, D.S.; Christian, M.H. Differential Impact of Climate Change on the Hydropower Economics of Two River Basins in High Mountain Asia. *Front. Environ. Sci.* **2020**, *8*, 26. [[CrossRef](#)]
25. Liu, C. Glacier Resources and Distributive Characteristics in the Central Asia Tianshan Mountains. *J. Glaciology Geocryol.* **1995**, *17*, 193–203.
26. Zhang, Z.; He, X.; Liu, L.; Li, Z.; Wang, P. Ecological Service Functions and Value Estimation of Glaciers in the Tianshan Mountains, China. *Acta Geogr. Sin.* **2018**, *73*, 856–867. [[CrossRef](#)]
27. Sorg, A.; Bolch, T.; Stoffel, M.; Solomina, O.; Beniston, M. Climate change impacts on glaciers and runoff in Tien Shan (Central Asia). *Nat. Clim. Chang.* **2012**, *2*, 725–731. [[CrossRef](#)]
28. Wang, X.; Yang, T.; Xu, C.-Y.; Yong, B.; Shi, P. Understanding the discharge regime of a glacierized alpine catchment in the Tianshan Mountains using an improved HBV-D hydrological model. *Glob. Planet. Chang.* **2019**, *172*, 211–222. [[CrossRef](#)]
29. Pfeffer, W.T.; Arendt, A.A.; Bliss, A.; Bolch, T.; Cogley, J.G.; Gardner, A.; Hagen, J.-O.; Hock, R.; Kaser, G.; Kienholz, C.; et al. The Randolph Glacier Inventory: A globally complete inventory of glaciers. *J. Glaciol.* **2014**, *60*, 537–552. [[CrossRef](#)]
30. Xing, W.; Li, Z.; Zhang, H.; Liang, P.; Zhang, M.; Mu, J. Spatial-Temporal Variation of Glacier Resources in Chinese Tianshan Mountains since 1959. *Acta Geogr. Sin.* **2017**, *72*, 1594–1605. [[CrossRef](#)]
31. Huss, M.; Hock, R. Global-Scale Hydrological Response to Future Glacier Mass Loss. *Nat. Clim. Chang.* **2018**, *8*, 135–140. [[CrossRef](#)]
32. Zhang, J.; Chun, X.; Yang, Q. Ndvi Variations and Its Response to Extreme Climate in Xinjiang Uygur Autonomous Region During 2001–2017. *Bull. Soil Water Conserv.* **2020**, *40*, 256–262, 281, 347. [[CrossRef](#)]
33. Hamed, K.H. Trend detection in hydrologic data: The Mann-Kendall trend test under the scaling hypothesis. *J. Hydrol.* **2008**, *349*, 350–363. [[CrossRef](#)]
34. Bo, S.; Li, Z.; Zhang, M.; Rong, G.; Xue, Y. A Comparative Study on Mass Balance between the Continental Glaciers and the Temperate Glaciers: Taking the Typical Glaciers in the Tianshan Mountains and the Alps as Examples. *J. Glaciol. Geocryol.* **2015**, *37*, 1131–1140. [[CrossRef](#)]
35. Yi, H.E.; Yang, T.B.; Juan, D.U.; Tian, H.Z. Glacier Variation of Past 22 Years in Alatau Mountains of Central Asia Based on Gis and Rs. *Res. Soil Water Conserv.* **2013**, *20*, 130–134.
36. Zhang, W.; Wang, N.; Xiang, L.I.; Liu, K. Glacier Changes and Its Response to Climate Change in the Gilgit River Basin, Western Karakorum Mountains over the Past 20 Years. *Mt. Res.* **2019**, *37*, 347–358.
37. Smith, T.; Bookhagen, B. Assessing Multi-Temporal Snow-Volume Trends in High Mountain Asia From 1987 to 2016 Using High-Resolution Passive Microwave Data. *Front. Earth Sci.* **2020**, *8*, 392. [[CrossRef](#)]
38. Kogutenko, L.; Severskiy, I.; Shahgedanova, M.; Lin, B. Change in the Extent of Glaciers and Glacier Runoff in the Chinese Sector of the Ile River Basin between 1962 and 2012. *Water* **2019**, *11*, 1668. [[CrossRef](#)]
39. Di Marco, N.; Avesani, D.; Righetti, M.; Zaramella, M.; Majone, B.; Borga, M. Reducing hydrological modelling uncertainty by using MODIS snow cover data and a topography-based distribution function snowmelt model. *J. Hydrol.* **2021**, *599*, 126020. [[CrossRef](#)]
40. Deng, H.; Chen, Y. The Glacier and Snow Variations and Their Impact on Water Resources in Mountain Regions: A Case Study in Tianshan Mountains of Central Asia. *Acta Geogr. Sin.* **2018**, *73*, 1309–1323. [[CrossRef](#)]
41. Xu, L.; Li, P.; Li, Z.; Zhang, Z.; Wang, P.; Xu, C. Advances in Research on Changes and Effects of Glaciers in Xinjiang Mountains. *Adv. Water Sci.* **2020**, *31*, 946–959. [[CrossRef](#)]
42. Zhao, Q.D.; Bai-Sheng, Y.E.; Ding, Y.J.; Zhang, S.Q.; Wang, J.; Wang, Z.R. Hydrological Process of a Typical Catchment in Cold Region: Simulation and Analysis. *J. Glaciol. Geocryol.* **2011**, *33*, 595–605.
43. Shen, Y.P.; Wang, G.Y.; Ding, Y.J.; Mao, W.Y.; Liu, S.Y.; Wang, S.D.; Mamatkanov, D.M. Changes in Glacier Mass Balance in Watershed of Sary Jaz-Kumarik Rivers of Tianshan Mountains in 1957–2006 and Their Impact on Water Resources and Trend to End of the 21th Century. *J. Glaciol. Geocryol.* **2009**, *31*, 792–800.
44. Wang, X.; Sun, L.; Zhang, Y.; Luo, Y. Estimation of Glacier Melt Contribution to Streamflow Using a Distributed Hydrologic Model for the Kumarik River, Tien Shan. *Resour. Sci.* **2015**, *37*, 475–484.
45. Gao, Q.Z.; Wang, R.; Giese, E. Impact of Climate Change on Surface Runoff of Tarim River Originating from the South Slopes of the Tianshan Mountains. *J. Glaciol. Geocryol.* **2008**, *30*, 1–11.
46. Sabit, M.; Rusul, Y.; Sulayman, A. Analysis of Water Resources and It's Hydrological Characteristics of Weigan River Basin. *J. Mt. Res.* **2003**, *2*, 195–200. [[CrossRef](#)]

47. Zhao, G.; Zhang, Z.; Liu, L.; Xu, L.; Wang, P.; Li, L.; Ning, S. Changes of Glacier Mass Balance in Manas River Basin Based on Multi-Source Remote Sensing Data. *Acta Geogr. Sin.* **2020**, *75*, 98–112. [[CrossRef](#)]
48. Li, J. Ice and Snow Water Resources and Runoff Frequency in Urumqi River and Mountain Area. *Bimon. Xinjiang Meteorol.* **2002**, *25*, 30–33. [[CrossRef](#)]
49. Duan, J.J.; Cao, X.L.; Shen, Y.P.; Gao, Q.Z.; Wang, S.D. Surface Water Resources and Its Trends in Weigan River Basin on the South Slope of Tianshan, China during 1956–2007. *J. Glaciol. Geocryol.* **2010**, *32*, 1211–1219.
50. Wang, S.; Xie, Z.; Li, Q. Comparison Study of Glacier Variations in East and West Tianshan Mountains. *J. Glaciol. Geocryol.* **2008**, *30*, 946–953.
51. Farinotti, D.; Longuevergne, L.; Moholdt, G.; Duethmann, D.; Mölg, T.; Bolch, T.; Vorogushyn, S.; Güntner, A. Substantial glacier mass loss in the Tien Shan over the past 50 years. *Nat. Geosci.* **2015**, *8*, 716–722. [[CrossRef](#)]
52. Farinotti, D.; Immerzeel, W.W.; De Kok, R.J.; Quincey, D.J.; Dehecq, A. Manifestations and Mechanisms of the Karakoram Glacier Anomaly. *Nat. Geosci.* **2020**, *13*, 8–16. [[CrossRef](#)] [[PubMed](#)]
53. Zhang, H.; Li, W.; Li, W. Influence of Late Springtime Surface Sensible Heat Flux Anomalies over the Tibetan and Iranian Plateaus on the Location of the South Asian High in Early Summer. *Adv. Atmos. Sci.* **2018**, *36*, 93–103. [[CrossRef](#)]
54. Gao, X.; Ye, B.; Zhang, S.; Qiao, C.; Zhang, X. Glacier Runoff Variation and Its Influence on River Runoff During 1961–2006 in the Tarim River Basin, China. *Sci. China Earth Sci.* **2010**, *53*, 880–891. [[CrossRef](#)]
55. Shen, Y.P.; Su, H.C.; Wang, G.Y.; Mao, W.M.; Li, Z.Q. The Responses of Glaciers and Snow Cover to Climate Change in Xinjiang (I): Hydrological Effects. *J. Glaciol. Geocryol.* **2013**, *35*, 513–527. [[CrossRef](#)]
56. Li, K.; Li, Z.; Gao, W.; Wang, L. Recent Glacial Retreat and Its Effect on Water Resources in Eastern Xinjiang. *Chin. Sci. Bull.* **2011**, *56*, 2708–2716. [[CrossRef](#)]